Biogeosciences Discuss., 9, 5011–5048, 2012
www.biogeosciences-discuss.net/9/5011/2012/
doi:10.5194/bgd-9-5011-2012

Biogeosciences Discussions

Description of the biogeochemical features of the subtropical southeastern Atlantic and the Southern Ocean south off South Africa during the austral summer of the International Polar Year

F. A. C. Le Moigne[1,*], **M. Boye**[1], **A. Masson**[1], **R. Corvaisier**[1], **E. Grossteffan**[2], **A. Guéneugues**[1], **and P. Pondaven**[1]

[1]Institut Universitaire Européen de la Mer, Technopole (IUEM) UMS3113, Laboratoire des Sciences de l'Environnement Marin (LEMAR, CNRS UMR6539), Brest-Iroise, 29280 Plouzané, France
[2]Unité Mixte de Services (UMS3113), Institut Universitaire Européen de la Mer, Technopole Brest-Iroise, 29280 Plouzane, France
[*]present address: Ocean Biogeochemistry and Ecosystem, National Oceanography Centre, European Way, Southampton SO14 3ZH, UK

Received: 19 January 2012 – Accepted: 3 April 2012 – Published: 25 April 2012

Correspondence to: F. A. C. Le Moigne (f.lemoigne@noc.soton.ac.uk)

Published by Copernicus Publications on behalf of the European Geosciences Union.

Abstract

Meridional and vertical distributions of several biogeochemical parameters were studied along a section in the southeastern Atlantic and the Southern Ocean south of South Africa during the austral summer 2008 of the International Polar Year to characterize the biogeochemical provinces and to assess the seasonal net diatom production. Based on analyses of macro-nutrients, ammonium (NH_4), chlorophyll *a*, (chl *a*) phaeopigments, biogenic silica (BSi), particulate inorganic carbon (PIC), and particulate organic carbon and nitrogen (POC and PON, respectively) four biogeochemical domains were distinguished along the section: the subtropical Atlantic, the confluence zone of the subtropical and subantarctic domains, the Polar Frontal Zone (PFZ) in the Antarctic Circumpolar Current (ACC) and the north-eastern branch of the Weddell Gyre. The subtropical region displayed extremely low nutrient concentrations featuring oligotrophic conditions, and sub-surface maxima of chl *a* and phaeopigments never exceeded, 0.5 $\mu g\, l^{-1}$ and 0.25 $\mu g\, l^{-1}$ respectively. The anticyclonic and cyclonic eddies crossed in the Cape Basin were characterized by a deepening and a rise, respectively, of the nutrients isolines. Mesoscale eddies can bring episodic pulse of nutrients into the photic zone. The confluence zone of the subtropical domain and the northern side of the ACC within the subantarctic domain displayed remnant nitrate and phosphate levels, whereas silicate concentrations kept to extremely low levels. In this area chl *a* level of 0.4–0.5 $\mu g\, l^{-1}$ distributed homogenously within the mixed layer, and POC and PON accumulated to values up to 10 µM and 1.5 µM, respectively; still indicative of biomass accumulation along the confluence zone during the late productive period. In the ACC domain, the Polar Frontal Zone was marked by a postbloom of diatoms that extended beyond the Polar Front (PF) during this late summer condition, as primarily evidenced by the massive depletion of silicic acid in the surface waters. The accumulation of NH_4 to values up to 1.25 µM at 100 m depth centred on the PF and the accumulation of BSi up to 0.5 µM in the surface waters of the central part of the PFZ also featured a late stage of the seasonal diatom bloom. Similar southward displacement of the silicic acid

depletion beyond the PF has been previously observed throughout the productive period, associated with the development and extension of the seasonal bloom of diatoms. The silica daily net production rate based on the seasonal depletion of silicic acid was estimated to be $11.9 \pm 6.5\,\mathrm{mmol\,m^{-2}\,d^{-1}}$ in the domain of the vast diatom post-bloom, agreeing well with the previously recorded values in this province. The Weddell Gyre occasionally displayed relative surface depletion of silicic acid suggesting a late stage of a relatively minor diatom bloom, possibly driven by iceberg drifting releases of iron. An accumulation of BSi up to 0.5 µM was recorded in the top 350 m of the southern branch of the ACC and in the Weddell Gyre which may be seen as the presence of heavily silicified diatoms due to lack of iron in this HNLC area. In this domain the estimated range of silica daily net production rate (e.g. $21.1 \pm 8.8\,\mathrm{mmol\,m^{-2}\,d^{-1}}$) is consistent with previous studies, but was not significantly higher than that in the Polar Front region.

1 Introduction

The Southern Ocean is deemed to play an important role in the global carbon cycle due to unique features involving both physical circulation and biological processes. In particular, the outcropping of deep water masses allows for the exchange of gases such as carbon dioxide (CO_2) between the deep sea and the atmosphere, while the incomplete utilisation of nutrients by the marine phytoplankton in this High-Nutrient Low-Chlorophyll (HNLC) area of the world ocean allows the concentration of CO_2 in the atmosphere to be substantially greater than would be the case if nitrate was used efficiently. Furthermore, the polar-extrapolar communication of heat, freshwater and CO_2 helps to close the hydrological cycle through the production of Antarctic Intermediate Water (AAIW) and Subantarctic Mode Water (SAMW). These water masses transport nutrients northward within the thermocline: by vertical mixing and advection, nutrients can sustain a large part of the primary and export productions at the low latitudes (Sarmiento et al., 2004). The formation of AAIW, SAMW and Antarctic Bottom Water

BGD
9, 5011–5048, 2012
Description of the biogeochemical features
F. A. C. Le Moigne et al.

(AABW) can also provide a mechanism for uptake and transport of anthropogenic CO_2 (Caldeira and Duffy, 2000). Models indicate that the response of the Southern Ocean to the global warming will be a critical factor determining the future uptake of anthropogenic CO_2 by the ocean (Sarmiento and Toggweiler, 1984). However the Southern Ocean is not a single vast biogeochemical system. For instance biogeochemical divides separate the Antarctic domain where the air-sea balance of CO_2 can be mainly controlled by the biological pump and circulation in the Antarctic deep-waters formation region, from the Subantarctic province where the global export production can be driven by the biological pump and the circulation in the region of the formation of AAIW and SAMW (Marinov et al., 2006). The conception of the Southern Ocean also evolved into several complex sub-systems, some of which are highly productive whilst others remain biologically poor all year long (Tréguer and Jacques, 1992).

At first glance the development and accumulation of phytoplankton biomass in the Southern Ocean are mainly controlled by the light intensity (Nelson and Smith, 1991), the availability of trace elements especially iron (Martin, 1990) and grazing pressure (Buma et al., 1991; Frost, 1996). However in the beginning of the productive period, biomass maxima concentrate along the Polar Front (Quéguiner et al., 1997), and at the confluence zone of the Subantarctic Front (SAF) and the Subtropical Front (STF) (Banse, 1991), benefiting from favourable and seasonal growth conditions in those regions. The bloom of large heavily silicified diatoms developing in late spring in the Polar Front region (Bathmann et al., 1997) leads to a massive depletion in silicic acid (Quéguiner et al., 1997), and to biogenic silica burial especially just south of the Polar Front (DeMaster, 1981). The export production in the spring bloom and the burial of biogenic silica in the Antarctic deep sea occur with very little coexisting organic matter (DeMaster et al., 1991; Ragueneau et al., 2002). The phytoplankton production of organic material is supported by the consumption of the macronutrients such as nitrate, phosphate and silicate (Koeve and Ducklow, 2001) and additional trace elements, such as iron (Martin et al., 1990), as well as light. Production should therefore be limited

BGD
9, 5011–5048, 2012

to that which can be supported by the annual supply of inorganic nutrients and trace elements to the euphotic zone.

The subtropical south-eastern Atlantic gyre is deemed to be an intense inter-ocean exchange area (Lutjeharms et al., 2003). Most of the leakage between the Indian Ocean and the South Atlantic indeed takes place within the retroflection of the Agulhas current where large eddies are translated to the Atlantic ocean (Lutjeharms and Vanballegooyen, 1988; Gladyshev et al., 2008). However, the biogeochemical functioning of this domain is understudied and requires more investigation. For instance, nutrients levels such as silicic acid, nitrate and phosphate may be extremely low, typical of an oligotrophic region (Longhurst, 1991). Furthermore the accumulation of nutrients and Chlorophyll *a* generally follow the general patterns set by currents and meandering in this region (Lutjeharms and Vanballegooyen 1988).

In this work we describe the biogeochemical functioning of the south-eastern Atlantic Ocean and the Southern Ocean south off South Africa based on the distributions of silicic acid, nitrate, phosphate, ammonium, chlorophyll *a*, phaeopigments, particulate organic carbon (POC), particulate organic nitrogen (PON), particulate inorganic carbon (PIC) and biogenic silica (BSi) along a section from the subtropical domain to the Weddell Sea Gyre along the Greenwich Meridian during the late austral summer of the 2008 International Polar Year.

2 Sampling and analytical procedures

2.1 Sampling

Samples were collected during the multidisciplinary MD166 BONUS-GoodHope cruise that took place during the International Polar Year in the austral summer 2008 (13 February 2008–24 March 2008) on board the French R/V *Marion-Dufresne II* sailing from Cape Town, South Africa, to 57° S along the Greenwich Meridian in the Southern Ocean (Fig. 1). The distribution of silicic acid, nitrate, phosphate, ammonium,

BGD
9, 5011–5048, 2012

chlorophyll *a* (chl *a*) and phaeopigments was studied at 78 stations along the section from surface to 5000 m depth (Fig. 2), and in the upper 300 m for ammonium, chl *a* and phaeopigments (Figs. 3–4). Particulate stocks of organic carbon (POC) and nitrogen (PON), and inorganic carbon (PIC) were sampled at 68 stations in the upper 300 m along the transect, whereas those of biogenic silica (BSi) were sampled at 12 stations (Fig. 5). The resolution between two stations varied between 20 and 40 nautical miles. The samples were collected using a CTD-rosette (SBE 32 Seabird) equipped with Niskin bottles. Potential temperature (Θ), salinity (*S*) and dissolved oxygen (O_2) were recorded using SBE 911+ Seabird probe, with, SBE3+, SBE4 and SBE43 sensors respectively (Branellec et al., 2010).

2.2 Analytical procedures

2.2.1 Nutrients and ammonium

Silicate, nitrate, phosphate and ammonium concentrations were measured on board the ship. Silicate and nitrate were analysed by standard method with a Bran+Luebbe AAIII auto-analyser as described by Tréguer and Le Corre (1979). Samples were run versus daily prepared standards diluted from stock standard solutions in artificial seawater. Phosphate was determined manually using a spectrophotometer (Shimatzu UV 1700) as described by Murphy and Riley (1962). Ammonium was analysed manually by spectrophotometry method (Shimatzu UV 1700) as described by Koroleff (1969). The detection limit for silicate, nitrate, phosphate and ammonium analyses was respectively, 0.1 µM, 0.04 µM, 0.05 µM and 0.05 µM.

2.2.2 Chlorophyll *a* and phaeopigments

Chlorophyll *a* (chl *a*) and phaeopigments were determined after filtration of 1–2 l of seawater on GF/F filters using a vacuum pump. The filters were placed in 90 % (*v*/*v*) acetone/water and homogenized in a cell for a minimum of 4 h followed by a

BGD
9, 5011–5048, 2012

centrifugation. Chlorophyll *a* level was then measured by fluorescence detection using a TURNER Design 10-AN Fluorimeter. Phaeopigment concentration was determined in these samples after the addition of 100 µM HCl (1N) (Strickland and Parsons, 1972). Filters were measured within a few days after their collection on board. Detection limit of the measurement of chlorophyll *a* and phaeopigment were respectively 0.005 $\mu g\,l^{-1}$ and 0.075 $\mu g\,l^{-1}$. Chlorophyll *a* analyses were calibrated versus a pure Chlorophyll *a* from spinach (Sigma).

2.2.3 Particulate matter

Total Particulate Carbon (TPC), Particulate Organic Carbon (POC) and Particulate Organic Nitrogen (PON) were analysed from a bulk of 2 l seawater filtered on 4 precombusted glass fiber filters (Whatman GF/F), as two filters were used for duplicate TPC determination and the others two for POC and PON duplicate analyses. The filters were kept frozen (–20 °C) before their analyses in the shore-based laboratory. POC and PON were analysed after fuming of the filter by acidic (HCl) smokes for 4 h in a dessicator and drying at 60 °C in an oven (Lorrain et al., 2003). POC and PON were measured using Carlo Erba Analyzer 1500. TPC was analysed using the same protocol and method, but without fuming the filters. The particulate inorganic carbon (PIC) concentrations were estimated from the difference between TPC and POC.

Biogenic silica (BSi) was determined on the retentive of 1 l seawater filtered onto polycarbonate filters (0.6 µm pore-size, diameter 47 mm) and the filters were dried off at 60 °C and stored for further analysis. Before analyses the filters were dried at 60 °C for 24 h and then kept at room temperature. BSi was analysed after the digestion of the filter with 0.2 M NaOH for 45 min at 100 °C (Ragueneau et al., 2005).

BGD
9, 5011–5048, 2012

3 Results

3.1 Hydrography

The section crossed in the north the subtropical domain extended southward to the southern branch of the Subtropical Front (S-STF) (Belkin and Gordon, 1996) at ~42°2′ S. Southward it crossed the Antarctic Circumpolar Current (ACC) bounded in the north by the S-STF and in the south by the Southern Boundary of the ACC (SBdy; Orsi et al., 1995) at ~55°54.3′ S, and then the region of the Weddell Sea Gyre at the southern end of the section (Fig. 1). Within the ACC, the subantarctic domain is bounded in the south by the Subantarctic Front (SAF; Orsi et al., 1995; Gordon et al., 1992) which was located at 44°2′ S, the Polar Frontal Zone (PFZ) is bounded in the south by the Polar Front (PF) at 50°22.4′ S. The Southern ACC Front (SACCF) was located at ~51°52′ S and the Southern Boundary of the ACC (SBdy) at ~55°54′ S. The mixed layer depth deepened southward from around 50 m in the subtropical and subantarctic zones, to 60 m in the Polar Frontal Zone, to 88 m in the southern side of the ACC and down to 90 m in the Weddell Gyre.

The subtropical domain was characterized by a turbulent dynamical regime commonly observed in this region (Gladyshev et al., 2008). Warm and salty anticyclonic eddies commonly interact strongly with slope waters, cyclonic eddies and South Atlantic waters. The anticyclonic eddies are generally referred as Agulhas rings and are ejected from the western boundary current of the South Indian Ocean, the Agulhas Current, at its retroflection (Lutjeharms and Vanballegooyen, 1988). During the expedition, two large eddies of subtropical origin were intersected in the subantarctic zone (Arhan et al., 2011). A cyclonic eddy (S) was crossed just south of the S-STF (at station 39) and was marked by pronounced low oxygen and CFCs anomalies revealing an origin at the South Africa continental slope (Arhan et al., 2011). In addition a large and intense anticyclonic eddy (M) that was an Agulhas ring had crossed the Agulhas Ridge and was observed adjacent to the SAF (at station 46; Arhan et al., 2011). In this domain Antarctic Intermediate Waters originated from the Indian Ocean (I-AAIW; Gordon

BGD
9, 5011–5048, 2012

et al., 1992) were depicted between 800 and 1200 m closer to Africa. Another variety of AAIW was observed to the south featuring the AAIW formed in the subantarctic domain of the southwest Atlantic (A-AAIW; Piola and Gordon, 1989). Deeper, centred at about 2500 m, a diluted variety of North Atlantic Deep Water which has flowed along the southwest African continental shelf (SE-NADW; Arhan et al., 2003) has been identified north of S-STF. At the bottom, an old variety of Antarctic Bottom Water (AABW) likely formed in the Weddell Sea (Reid, 1989; Gladyshev et al., 2008) was observed in the Cape Basin abyssal plain below 3500 m depth, characterized by low salinity and cold temperature.

In the ACC domain south of the Agulhas Ridge, the Surface Water (SW) was marked by a southward decrease of temperature from 4 °C to 2 °C. Below lays the Atlantic variety of AAIW (A-AAIW) which subducts along the SAF. The A-AAIW waters were detected between depths of 300 and 600 m. At greater depths the Upper Circumpolar Deep Water originated from the southwest Atlantic (A-UCDW; Whitworth and Nowlin, 1987) was depicted north of the PF at about 1000–1500 m. North of the PF, the deeper waters (1500–3000 m) exhibited properties of diluted South West NADW (SW-NADW), which flows along the continental slope of South America, down to the Argentinean Basin before being injected in the ACC in the southwestern Atlantic (Whitworth and Nowlin, 1987). At the bottom a variety of fresher and colder bottom water than AABW depicted in the Cape Abyssal plain was found below 3250 m on the northern flank of the Mid Atlantic Ridge. South of the PF, deep waters exhibited properties of UCDW which has passed through the Drake Passage (DP-UCDW; Whitworth and Nowlin, 1987) between 250 and 700 m and deeper those of Lower Circumpolar Deep Water (LCDW) with lower salinity than SW-NADW. South of the ACC domain, the whole water column was impacted by waters of the Weddell Gyre: those waters are much colder and those near the bottom were a younger variety of AABW than those observed in the Cape Basin, as they are characterized by higher dissolved O_2 concentrations. Winter Water (WW) was detected in the ACC domain and the Weddell Gyre between 100 and 250 m with temperature below 1 °C.

BGD
9, 5011–5048, 2012

3.2 Nutrients

The concentrations of nitrate, silicate and phosphate increased with depth, remarkably in the subtropical region and slightly in the Southern Ocean (Fig. 2), featuring nutrient-type distributions with biological uptake in surface waters and remineralisation in deeper waters even if the nutrient biological uptake is significantly reduced south of the Polar Front. Nitrate distribution showed a meridional gradient in the surface waters with a southward increase from sub-micromolar levels in the subtropical domain up to 30 µM at the Polar Front and beyond (Fig. 2). Phosphate also followed a southward increase from sub-micromolar values in the subtropical domain, to 1.75 µM at the Polar Front, and up to 2 µM south of 52° S (Fig. 2). On the other hand, the concentrations of silicate kept to low values (sub-micromolar range) from the subtropical domain towards the southern side of the Polar Front, beyond which they increased up to 75 µM in the southern side of the ACC (Fig. 2). Nitrate and phosphate concentrations started to increase southward in the subantarctic domain, while silicate concentrations started to increase south of the Polar Front (Fig. 2).

Among other specific features of nutrients distribution, a bowl-shaped feature in the silicate, nitrate and phosphate profiles that extended down to about 800 m was observed between the S-STF and the SAF at 44° S south of the Agulhas ridge, corresponding to the core of the anticyclonic eddy-M (Fig. 2). Furthermore, silicate isoclines were deepening northward from the PF (Fig. 2).

Relatively low nutrients concentrations were recorded at depth within the core of the SE-NADW observed from 33° S to 44° S between roughly 2000 and 4000 depth (Fig. 2), with concentrations of 60 µM for silicate, 1.75 µM for phosphate and 27 µM for nitrate. Silicate concentrations ranged from 10 to 20 µM in the A-AAIW, and nitrate and phosphate extended from 10 to 30 µM and 1 to 2 µM respectively. In the WW, nutrients concentrations ranges were similar to those recorded in the A-AAIW. Finally, silicate concentrations were relatively high (130 µM) in the core of the "old variety" of AABW depicted at roughly 36° S below 4000 m depth (Fig. 2).

BGD

9, 5011–5048, 2012

3.3 Ammonium

Ammonium concentrations were very low in the upper 250 m depth of the subtropical domain, within sub-micromolar range (Fig. 3). Subsurface maximum of about 1.25 µM was observed between 70 and 100 m centred on the Polar Front (Fig. 3). Persistent concentrations (e.g. 0.25–0.75 µM) extended northward of this maximum in the Polar Frontal Zone, and southward in the southern branch of the ACC (Fig. 3).

3.4 Chlorophyll *a* and phaeopigments

The chlorophyll *a* concentrations never exceed 0.5 µg l^{-1} in the surface waters along the section (Fig. 4). Sub-surface relative maxima (<0.4 µg l^{-1}) were less and less deep southward along the subtropical region (Fig. 4), and chl *a* accumulated in the top 50 m with a relative maximum of chl *a* (~0.5 µg l^{-1}) observed at 25 m along the confluence of the subtropical and the subantarctic zones (Fig. 4). In the Polar Frontal Zone the chlorophyll *a* concentration was about 0.3 µM in the upper 70 m (Fig. 4) corresponding to the mixed layer depth. The southern side of the ACC (between PF and SBby) was marked by extremely low chlorophyll *a* concentrations (0.1–0.2 µg l^{-1}), whereas they were slightly higher (0.3 µg l^{-1}) in the Weddell Gyre (Fig. 4). The distribution of the phaeopigments that are degradation products of the chlorophyll *a* also dispatched a subsurface maximum of 0.25 µg l^{-1} centred at around 25 m depth at the confluence of the subtropical and subantarctic domains (Fig. 4). The phaeopigment pattern followed similar southward trend as the chl *a* in these domains, with a subsurface maximum becoming a surface maximum (Fig. 4). In the Polar Frontal Zone the levels of phaeopigments were extremely low, of about 0.1 µg l^{-1} in the upper 70 m (Fig. 4). The concentrations were the lowest in the top 100 m in the southern side of the ACC, while relatively higher levels (0.6 µg l^{-1}) were recorded at about 100 m depth in the Weddell Gyre (Fig. 4).

BGD
9, 5011–5048, 2012

3.5 Particulate matter

3.5.1 Particulate organic carbon and nitrogen

The particulate organic carbon (POC) and the particulate organic nitrogen (PON) ranged from undetectable to 15 µM, and undetectable to 2 µM, respectively, in the mixed layers along the section (Fig. 5). The distribution of POC and PON displayed higher levels in surface waters than in deep waters (Fig. 5), where almost undetectable levels were observed below 100 m depth. The highest concentrations of POC and PON along the section were recorded in the upper 50 m along the confluence zone of the subtropical and subantarctic domain with respective concentrations of 15 µM and 2 µM (Fig. 5). POC and PON concentrations were lower south of the PF, of about 2.5–5 µM and 0.5 µM respectively; whereas POC levels were relatively higher at the SBdy and in the PFZ as compared to values recorded at the SACCF (Fig. 5).

3.5.2 Biogenic silica and particulate inorganic carbon

Biogenic silica (BSi) concentrations increased southward in the top 100 m, from below detection limit in the subtropical province to 0.5 µM in the Polar Frontal Zone (Fig. 5). Then the distribution was marked by extremely low concentrations in the top 350 m at the PF and its northern side (<0.2 µM), while BSi concentrations were slightly higher and fairly homogenous (at around 0.3 µM) in the upper 350 m between PF and SACCF (Fig. 5). Accumulation of BSi (0.55 µM) occurred south of the SACCF between 150 and 350 m (Fig. 5).

Particulate inorganic carbon (PIC) concentrations generally kept to low values (<4 µM) along the section. The largest accumulation of PIC (4 µM) was observed in the top 50 m on the southern side of the ACC and in the Weddell Gyre (Fig. 5). Lower relative accumulations were recorded in deeper waters (200–300 m) in the PFZ (2 µM), and in the upper 50 m (2 µM) and below 300 m depth (1 µM) in the northern part of the subtropical domain off the South African shelf.

4 Discussion

4.1 Biogeochemical features of the subtropical domain and its confluence with the subantarctic zone

Silicate, nitrate and phosphate concentrations were extremely low (<sub-micromolar level) in the upper 200 m of the subtropical region, and kept to low levels in the subantarctic domain despite a slight increase of nitrate and phosphate concentrations (Fig. 2). Such extremely low nutrients concentrations compared well with those previously observed at the same latitudes and season along 45° E (Table 2; Mohan et al., 2008), suggesting no significant variations of nutrient concentrations (and thereby gradients location) in the subantarctic domain between S-STF and SAF through the productive season.

In the subtropical domain, the subsurface relative maxima of chl *a* associated with the extremely low concentrations of nutrients (close to detection limit) suggested typical oligotrophic system conditions. It is likely that the ammonium which is kept at low value here was rapidly taken up. Oligotrophic conditions were further supported by ^{15}N incubation experiments which showed that the new production rate was low in this domain, unlike the regenerated production (Joubert et al., 2011). PIC and BSi concentrations were extremely very low in this area, the C and N biomass was therefore not a production of calcifying or silicifying phytoplankton. The production was more likely due to non-mineralizing organisms typical of an oligotrophic system. The radionuclids derived export production (e.g. $^{234}Th/^{238}U$) showed that the transfer rate of carbon to the mesopelagic zone was quite low in this domain (Planchon et al., 2012) consistent with a low new production (Joubert et al., 2011), and probably leading to the relative accumulation of particulate organic N and C observed in the subtropical region (Fig. 5). Our results supported that in the subtropical gyre south off South Africa, waters were strongly oligotrophic and production was sustained by recycling processes.

At the confluence zone of the subtropical and subantarctic domains, chl *a* and phaeopigments (degradation pigments) displayed their highest levels (Fig. 4), as well as particulate organic C and N (Fig. 5). The transition between the two domains was marked by a slight increase in nitrate and phosphate concentrations southward (Fig. 2). The accumulation of particulate organic material (Figs. 4–5) also occurred where the highest cell abundance was recorded along the section (Beker and Boye, 2010). Besides the nutrients nitrate and phosphate, the production was probably also sustained by iron which was not limiting in this frontal zone (Chever et al., 2010). The accumulation of material could also partly result from a low export rate as evidence by $^{234}Th/^{238}U$ measurements (Planchon et al., 2012), the biomass being remineralized within the mixed layer as further supported by an ammonium peak in this area (Fig. 3).

In the subantarctic zone the nutrients distribution appeared as upward pointing tongues of high values (and low values for CFCs; Arhan et al., 2011) in the core of the cyclonic eddy (Fig. 6a). However as the tongue-shaped patterns generally cross the density contours, these eddy anomalies were probably more than just an isopycnal uplift of properties, and reflected trapping and transport of distant water by the eddy (Arhan et al., 2011). The nutrients signatures of the Agulhas anticyclone ring observed adjacent to the SAF were characterized by pronounced low values at the core station down to ~600 m, relative to values at the surrounding stations (Fig. 6b) indicative of winter convection. Both eddies were found to transport subtropical water and illustrated the capacity of eddies to transfer subtropical and alongslope water properties, such as nutrients, into the subantarctic zone (Arhan et al., 2011). However, although mesoscale eddies episodically increase nutrient supply to relatively poor nutrient water, they may have an insignificant effect on export production and carbon sequestration (Benitez-Nelson and McGillicuddy, 2008).

In addition to mesoscale dynamics, nutrient distributions are driven by the large scale circulation and their signatures in deep waters can be used to better characterize the water-masses (Pollard et al., 2002). For instance the core of SE-NADW that flowed in the northern Cape Basin of the section, along the southwest African continental shelf (Arhan et al., 2003) was depicted by relative low nutrients values (e.g. nitrate $< 30\,\mu M$; phosphate $< 2\,\mu M$; silicate $< 60\,\mu M$), as well as by the salinity signature and

BGD
9, 5011–5048, 2012

oxygen maximum (Bown et al., 2011). In bottom waters the "old variety" of AABW was characterized, at around 36° S, by extremely high concentrations in silicate (Fig. 2) as previously observed at this latitude (Gladyshev et al., 2008). The high levels in silicate in this variety of AABW probably find its origin in the formation region of AABW close to the Antarctic shelf (Weddell and Ross seas) where this water body deepens with the imprint of high surface silicate levels. While deepening, this water which already has a high silicate content, is enriched in silicate thanks to exchanges with the Antarctic shelf which contains a lot of opal sediments (DeMaster, 2002).

4.2 Biogeochemical features of the central and southern Antarctic Circumpolar Current domain and the Weddell Gyre

4.2.1 The seasonal diatom bloom along the Polar Front

In the surface waters, the nutrients distributions all showed meridional gradients with a southward increase, whereas the location of the sharp increase differed for the silicate gradient compared to the nitrate and phosphate (Fig. 2). Indeed the highest gradient of silicate was located southward of the PF in this late summer conditions, while for nitrate and phosphate it was observed at the PF (Fig. 2), consistent with previous observations (Pollard et al., 2002). In the Polar Frontal Zone, silicate concentrations were lower in the late austral summer (this study) compared to spring (e.g. October 1992; Löscher, 1999), while nitrate and phosphate levels were on the same range (Table 2). It suggests that silicate is depleted over the productive season in the PFZ, unlike nitrate and phosphate. Similar southward move of the sharp gradient of silicate across the PF from spring towards late austral summer has already been observed in the Pacific sector of the Southern Ocean (Franck et al., 2000; Nelson et al., 2001). Conversely, the southern side of the ACC was marked by relatively high silicate levels (and high nitrate and phosphate) in the surface waters, with no seasonal variability (Table 2). The temporal and spatial variability of the silicate gradient in the vicinity of the PF are cause by the migration of the PF, and by the shifts in space and time of the production of the

BGD
9, 5011–5048, 2012

Antarctic diatoms (Bathmann et al., 1997; Pollard et al., 2002). Early spring blooms of large diatoms are indeed reported in the Polar Frontal Zone (Bathmann, 1998). These blooms cause the depletion of silicate in the Polar Frontal Zone over the productive season, hence resulting in the southward migration of the sharp gradient of silicate observed here in late summer. Besides the depletion of silicate (Fig. 2), the extremely low concentrations of chl *a* and phaeopigments reported here (Fig. 4) associated with the relative accumulation of ammonium (Fig. 3) further reflected a vast post-bloom of diatoms centred on the PF during the late summer conditions. The flourishing diatoms are heavy silicified due to iron limitation (De Baar et al., 1997), whereas their nitrate biological uptake may decrease (De La Rocha et al., 2000). This causes a strong depletion of silicate as compared to nitrate. In the surface waters of the diatoms post-boom area, the value of Si* (defined as [Si]-[NO_3]; Sarmiento et al., 2004) was indeed negative (Fig. 7), further suggesting a decoupling between the silicon and nitrogen export in the vicinity of the PF. These blooms generate intense flux of silicon towards the deep ocean. The biogenic silica is remineralised slowly in the deep ocean (Tréguer and Jacques, 1992), resulting in relatively high opal levels in the sediments of the Polar Frontal Zone (DeMaster, 1981). In this area BSi displayed a peculiar distribution with relatively high concentration in the central PFZ while at the PF, the concentrations were lower (Fig. 5). This may be linked to spatial differences in export and further remineralisation in the upper water column. Indeed ^{234}Th derived POC export indicated that the export was the greatest at about 51° S decreasing in both directions (Planchon et al., 2012). The intense export of material within the PF (mainly consisting of diatoms) fitted with the removal of BSi from the upper water column at this latitude (Fig. 5). POC and PON concentrations were also low (Fig. 5) emphasing efficient export as well at the PF. However BSi export was probably stoechiometrically higher than POC export there, as diatoms were likely limited by dissolved iron (Chever et al., 2010; De La Rocha et al., 2000) and would therefore be heavily silicified (De La Rocha et al., 2000). Anyway the combined export of BSi and POC can further support the ballast theory (Armstrong et al., 2002; Francois et al., 2002; Klaas and Archer, 2002) recently confirmed in the subarctic Pacific (Honda and Watanabe, 2010), another diatom dominated area.

The Antarctic Intermediate Water (AAIW) and Subantarctic Mode Water (SAMW) transport nutrients within the thermocline which can drive a large part of the primary and export production at low latitudes (Sarmiento et al., 2004). However the production of SAMW can be insignificant in the Atlantic sector of the Southern Ocean (Whitworth and Nowlin, 1987; McCartney, 1975), and the water masses encountered along the section did not reveal the occurrence of SAMW. By contrast the Atlantic variety of AAIW formed in the subantarctic region of the southwest Atlantic (A-AAIW; Piola and Gordon, 1989) was depicted in the ACC south of the Agulhas Ridge, as those waters subducted northward along the SAF (Arhan et al., 2011). These waters were also observed in the southern side of the subtropical domain (Arhan et al., 2011). These waters were characterized by negative Si* values ($<-10\,\mu$M; Fig. 7), reflecting the nutrient depletion of silicate (and to a lesser extend of nitrate) in the PFZ (Fig. 2) generated by the early spring diatom bloom. According to the model (Sarmiento et al., 2004), the negative Si* signature of the A-AAIW can lead to a decrease in export production outside the Southern Ocean as these waters likely fuel the low latitudes productivity with nutrients. Furthermore Si* is deemed to be an indicator of nutrient status related to the requirements of diatoms, provided Si:N ratio of non-starving diatoms (e.g. by light, macro- and micro-nutrients) is close to 1 (Brzezinski, 1985) which requires Si* ≥ 0 (Sarmiento et al., 2004). Thus the negative value of Si* recorded in the A-AAIW can provide indirect evidence of limiting conditions for diatom growth in the upper layers of the PFZ and PF regions. Surface dissolved iron concentrations were indeed low in these regions (e.g. < 0.2 nM; Chever et al., 2010), probably limiting the growth of Antarctic diatoms.

We have estimated a seasonal net silicate:nitrate (ΔSi:ΔNO_3^-) removal ratio (e.g. biological uptake minus regeneration) in the mixed layer of the ACC domain from 0.7:1 to 4.8:1 µM:µM (Fig. 8), based on the integrated silicate depletion (ΔSi) and nitrate depletion (ΔNO_3^-) given by their reference values in the Winter Waters present at the depth of the temperature minimum. The values observed in this domain were in the same ranges as those previously recorded in the Indian sector of the Southern Ocean (Le Corre and Minas, 1983), and in the Weddell Sea (Hoppema et al., 2007). Furthermore the values of the $\Delta Si:\Delta NO_3^-$ ratios estimated in the diatom post-bloom region were above 1 (Fig. 8), suggesting a lower seasonal net nitrate uptake as compared to that of silicate. This is in line with the decrease of nitrate uptake rate and the unaffected silicate uptake rate of diatoms observed in culture experiments under Fe-depleted conditions (De La Rocha et al., 2000). Nevertheless, the seasonal net nitrogen removal may be higher than that estimated for nitrate (ΔNO_3^-) due to the occurrence of ammonium and urea (e.g. regenerated production). Hence the seasonal net assimilation ratio $\Delta Si/\Delta NO_3^-$ estimated here would have been overestimated. For instance the ratios of new production over total nitrogen production (e.g. called "*f* ratio") have been estimated around 0.4 in the diatom post-bloom region (Joubert et al., 2011), indicating that the contribution of other forms of nitrogen such as urea and ammonium are likely to be significant. Next the silicate assimilation rates based on mixed layer mass balance were estimated at $3.0 \pm 0.8\,\mathrm{mol\,Si\,m^{-2}\,yr^{-1}}$ on average south of the PF (Fripiat et al., 2011). However, those authors suggested that their estimation can be underestimated due to the supply of dissolved silicon to the mixed layer during the stratification period. Therefore, the assimilation rate of silicate we estimated could also be significantly biased, and the seasonal net assimilation ratio $\Delta Si/\Delta NO_3$ could have been higher, still supporting lower seasonal net nitrate consumption as compared to that of silicate.

We estimated daily silica production rate (*P*Si) and nitrogen (*P*N) derived from the estimated seasonal net removal ratios and assuming the nutrients depletion by biological activity occurred over a productive period of 90 days in the Southern Ocean (e.g. November to February; Pondaven et al., 2000). The inputs of silicate and of nitrogen into the surface layer by vertical diffusion and by lateral advection were not considered in the calculation of *P*Si and *P*N, neither the production based on ammonium, urea or nitrite. On apropriate time scales, we assume that *P*Si and *P*N are valid estimation of the production of BSi and PON. The silica daily production rate estimated that way spreads from 1.5 to $55.5\,\mathrm{mmol\,m^{-2}\,d^{-1}}$ in the ACC domain (Fig. 9). These values are

BGD
9, 5011–5048, 2012

in the same range than those reported at these latitudes (Pondaven et al., 2000). *P*Si was slightly higher in the vicinity of the PF (Fig. 9), in line with the diatom post-bloom condition. Iron-limited Antarctic diatom blooms of *Fragilariopsis kerguelensis* reported at these latitudes in spring (Bathmann et al., 1997; de Baar et al., 1997) accumulate a large amount of silicate to grow, possibly accounting for the relatively higher *P*Si in the vicinity of the PF. Nevertheless, the silica daily production rates could have been underestimated by not taking into account additional Si external inputs in the surface waters. For instance the external supply of silicate to the mixed layer (*via* physical processes) south of the PF during the stratification period could account for a third of the net annual Si supply (Fripiat et al., 2011). The nitrogen daily production rate *P*N spreads from 1.0 to 19.2 $\mathrm{mmol\,m^{-2}\,d^{-1}}$ in surface waters of the ACC, with no significant meridional trend (Fig. 10). This range is similar to those reported at these latitudes (Pondaven et al., 2000). As already mentioned the nitrogen daily production rates may have been underestimated, since the regenerated production was not considered neither the external sources of nitrogen to the mixed layer. Recent studies into nitrification suggested that the nitrification can be significant in the photic zone (Yool et al., 2007).

4.2.2 The Weddell Gyre

Relatively high levels of BSi persisted in the upper water-column (Fig. 5), possibly suggesting a low dissolution rate of BSi leading to an accumulation of BSi. Another interesting feature of the northern branch of the Weddell gyre, is the relatively small depletion of silicate (e.g. Stations 103–104). This small depletion of silicate, associated with the slight increase of chl *a* and phaeopigments concentrations (Fig. 4) suggested a late stage of a relatively minor diatom bloom. Furthermore this diatom-dominated assemblage contained degraded frustules with small or absent chloroplasts (Becker and Boye, 2010), also suggesting a late stage of a diatom bloom. Production of diatoms has been already reported south of the SBdy (Arrigo et al., 1999).

Surface dissolved iron concentrations were however low in the north-eastern Weddell Gyre (e.g. <0.2 nM; Chever et al., 2010) likely limiting the Antarctic diatoms growth.

Hence it is possible that sea-ice melting stimulates the diatom production as recently suggested in the Weddell Sea (Smith et al., 2007), providing sea-ice can be source of iron to the surrounding waters (Boye et al., 2001; Lannuzel et al. 2008, Klunder et al. 2011) that can support local and episodic diatom production. In the Weddell Gyre, PSi and PN were similar compared to the ACC suggesting that consumption of Si and N were comparable on the seasonal timescale

5 Conclusions

Different biogeochemical provinces were identified in the south-eastern Atlantic and the Southern Ocean during the MD166 BONUS-GoodHope cruise based on the distribution of nutrients, ammonium, chl *a*, phaeopigments and particulate stocks. The subtropical region was characterized by oligotrophic conditions with extremely low nutrients concentrations. The confluence zone between the subtropical and the subantarctic domains was characterized by a relative maximum of sub-surface chl *a* and by the accumulation of particulate matter due to low export production and significant recycled production. In the ACC, the occurrence of a vast diatom post-bloom was depicted in the vicinity of the Polar Front during the late summer. The preferential removal of silicate by diatoms under iron-limited conditions as compared to that of nitrate in the post-bloom area can lead to the surface depletion of silicate and the southward migration of the silicate gradient beyond the Polar Front. Coupled biogenic silica production and accumulation throughout the water column suggested that dissolution has played a significant role in the silicon cycle in the ACC and the Weddell Gyre.

Finally, in the Weddell Gyre, the low consumption of silicate suggested a diatom post-bloom of small magnitude, which has been probably sustained by iron released from drifting icebergs whereas biogenic silica has accumulated in the upper water column probably due to low dissolution rate in these cold waters. However we do not sufficient information to support this hypothesis.

BGD
9, 5011–5048, 2012

Acknowledgements. We thank the captain and the crew of the French research vessel *Marion Dufresne II* for their wonderful work at sea during the IPY MD166 BONUS-GOODHOPE cruise. S. Speich (LPO, Brest, France) and M. Boye (LEMAR, Brest, France) were co-chief scientists of the cruise, and we thank as well as their collaborators M. Arhan (LPO, Brest, FR) and F. Dehairs (VUB, Brussels, Belgium). We are grateful to the colleagues of the nutrient CTD sampling team, and to Sebastien Aubin (LEMAR) for assisting biogenic silica analyses. This investigation was supported by the French LEFE National Program of INSU at CNRS, the National Agency of French Research (ANR-07-BLAN-0146-01) and the Paul Emile Victgor Institut (IPEV). F. Dehairs and Helen Griffin are also warmly acknowledged for improving the manuscript. This work was part of the Master degree research of F. A. C. L. M. It is a contribution to the International Polar Year and the international ICED programmes.

The publication of this article is financed by CNRS-INSU.

References

Arhan, M., Mercier, H., and Park, Y. H.: On the deep water circulation of the eastern south Atlantic ocean, Deep-Sea Res. Part I, 50, 889–916, doi:10.1016/s0967-0637(03)00072-4, 2003.

Arhan, M., Speich, S., Messager, C., Dencausse, G., Fine, R. A., and Boye, M.: Anticyclonic and cyclonic eddies of subtropical origin in the subantarctic zone south of Africa, J. Geophys. Res., 116, C11004, doi:10.1029/2011JC007140, 2011.

Armstrong, R. A., Lee, C., Hedges, J. I., Honjo, S., and Wakeham, S. G.: A new, mechanistic model for organic carbon fluxes in the ocean based on the quantitative association of POC with ballast minerals, Deep-Sea Res. Part II, 49, 219–236, 2002.

Arrigo, K. R., Robinson, D. H., Worthen, D. L., Dunbar, R. B., DiTullio, G. R., VanWoert, M., and Lizotte, M. P.: Phytoplankton community structure and the drawdown of nutrients and CO_2 in the southern ocean, Science, 283, 365–367, 1999.
Banse, K.: Iron availability, nitrate uptake, and exportable new production in the sub-arctic pacific, J. Geophys. Res.-Oceans, 96, 741–748, 1991.
Bathmann, U. V.: Ecology and biogeochemistry in the atlantic sector of the southern ocean during austral spring: The first jgofs expedition aboard rv "polarstern", J. Marine Syst., 17, 77–85, 1998.
Beker, B. and Boye, M.: Phytoplankton assemblages in the Southern Ocean during the International Polar Year. Ocean Sciences Meeting, 22–26 February 2010, Portland, USA, 2010.
Bathmann, U. V., Scharek, R., Klaas, C., Dubischar, C. D., and Smetacek, V.: Spring development of phytoplankton biomass and composition in major water masses of the atlantic sector of the southern ocean, Deep-Sea Res. II, 44, 51–67, 1997.
Belkin, I. M. and Gordon, A. L.: Southern ocean fronts from the greenwich meridian to tasmania, J. Geophys. Res.-Oceans, 101, 3675–3696, 1996.
Benitez-Nelson, C. R. and McGillicuddy, D. J.: Mesoscale physical-biological-biogeochemical linkages in the open ocean: An introduction to the results of the e-flux and eddies programs – preface, Deep-Sea Res. II, 55, 1133–1138, doi:10.1016/j.dsr2.2008.03.001, 2008.
Bowie, A. R., Maldonado, M. T., Frew, R. D., Croot, P. L., Achterberg, E. P., Mantoura, R. F. C., Worsfold, P. J., Law, C. S., and Boyd, P. W.: The fate of added iron during a mesoscale fertilisation experiment in the Southern Ocean, Deep-Sea Res. II, 48, 2703–2743, 2001.
Bown, J., Boye, M., Baker, A., Duvieilbourg, E., Lacan, F., Le Moigne, F., Planchon, F., Speich, S., and Nelson, D. M.: The biogeochemical cycle of dissolved cobalt in the Atlantic and the Southern Ocean south off the coast of south Africa, Mar. Chem., 126, 193–206, 2011.
Boye, M., Van den Berg, C. M. G., De Jong, J. T. M., Leach, H., Croot, P., and De Baar, H. J.: Organic complexation of iron in the southern ocean, Deep Sea Res., 48, 1477–1497, 2001.
Branellec, P., Arhan, M., and Speich, S.: Projet goodhope, campagne bonus-goodhope, rapport de donnees ctd-o2, Rapport interne IFREMER, OPS/LPO10-02, 2010.
Brzezinski, M. A.: The si-c-n ratio of marine diatoms – interspecific variability and the effect of some environmental variables, J. Phycol., 21, 347–357, 1985.
Buma, A. G. J., Debaar, H. J. W., Nolting, R. F., and Vanbennekom, A. J.: Metal enrichment experiments in the weddell-scotia seas – effects of iron and manganese on various plankton communities, Limnol. Oceanogr., 36, 1865–1878, 1991.

BGD
9, 5011–5048, 2012

Description of the biogeochemical features

F. A. C. Le Moigne et al.

Caldeira, K. and Duffy, P. B.: The role of the southern ocean in uptake and storage of anthropogenic carbon dioxide, Science, 287, 620–622, 2000.
Chever, F., Bucciarelli, E., Sarthou, G., Speich, S., Arhan, M., Penven, P., and Tagliabue, A.: Physical speciation of iron in the atlantic sector of the Southern Ocean along a transect from the subtropical domain to the Weddell Sea gyre, J. Geophys. Res., 115, doi:10.1029/2009JC005880, 2010.
de Baar, H. J. W., VanLeeuwe, M. A., Scharek, R., Goeyens, L., Bakker, K. M. J., and Fritsche, P.: Nutrient anomalies in Fragilariopsis kerguelensis blooms, iron deficiency and the nitrate/phosphate ratio (a.c. Redfield) of the Antarctic Ocean, Deep-Sea Res. II, 44, 229–260, 1997.
De La Rocha, C. L., Hutchins, D. A., Brzezinski, M. A., and Zhang, Y. H.: Effects of iron and zinc deficiency on elemental composition and silica production by diatoms, Mar. Ecol.-Prog. Ser., 195, 71–79, 2000.
DeMaster, D. J.: The supply and accumulation of silica in the marine environment, Geochim. Cosmochim. Acta, 45, 1715–1732, 1981.
DeMaster, D. J., Brewster, D. C., McKee, B. A., and Nittrouer, C. A.: Rates of particle scavenging, sediment reworking, and longitudinal ripple formation at the hebble site based on measurements of 234th and 210pb, Mar. Geol., 99, 423–444, 1991.
Franck, V. M., Brzezinski, M. A., Coale, K. H., and Nelson, D. M.: Iron and silicic acid concentrations regulate si uptake north and south of the polar frontal zone in the pacific sector of the southern ocean, Deep-Sea Res. II, 47, 3315–3338, 2000.
Francois, R., Honjo, S., Krishfield, R., and Manganini, S.: Factors controlling the flux of organic carbon to the bathypelagic zone of the ocean, Global Biogeochem. Cy., 16, 1087, doi:10.1029/2001gb001722, 2002.
Fripiat, F., Cavagna, A.-J., Dehairs, F., Speich, S., André, L., and Cardinal, D.: Silicon pool dynamics and biogenic silica export in the Southern Ocean inferred from Si-isotopes, Ocean Sci., 7, 533–547, doi:10.5194/os-7-533-2011, 2011.
Frost, B. W.: Phytoplankton bloom on iron rations, Nature, 383, 475–476, 1996.
Gladyshev, S., Arhan, M., Sokov, A., and Speich, S.: A hydrographic section from south africa to the southern limit of the antarctic circumpolar current at the greenwich meridian, Deep-Sea Res. I, 55, 1284–1303, doi:10.1016/j.dsr.2008.05.009, 2008.

BGD
9, 5011–5048, 2012

F. A. C. Le Moigne et al.

Gordon, A. L., Weiss, R. F., Smethie, W. M., and Warner, M. J.: Thermocline and intermediate water communication between the south-Atlantic and Indian oceans, J. Geophys. Res.-Oceans, 97, 7223–7240, 1992.

Honda, M., and Watanabe, S.: Importance of biogenic opal as ballast of particulate organic carbon (POC) transport and existence of mineral ballast-associated and residual POC in the western Pacific Subarctic Gyre, Geophys. Res. Lett., 37, L02605, doi:10.1029/2009GL041521, 2010.

Hoppema, M., Middag, R., de Baar, H. J. W., Fahrbach, E., van Weerlee, E. M., and Thomas, H.: Whole season net community production in the weddell sea, Polar Biol., 31, 101–111, doi:10.1007/s00300-007-0336-5, 2007.

Joubert, W. R., Thomalla, S. J., Waldron, H. N., Lucas, M. I., Boye, M., Le Moigne, F. A. C., Planchon, F., and Speich, S.: Nitrogen uptake by phytoplankton in the Atlantic sector of the Southern Ocean during late austral summer, Biogeosciences, 8, 2947–2959, doi:10.5194/bg-8-2947-2011, 2011.

Klaas, C. and Archer, D. E.: Association of sinking organic matter with various types of mineral ballast in the deep sea: Implications for the rain ratio, Global Biogeochemical Cycles, 16, 1116, doi:10.1029/2001gb001765, 2002.

Klunder, M. B., Laan, P., Middag, R., de Baar, H. J. W., and van Ooijen, J. C.: Dissolved Fe in the Southern Ocean (Atlantic sector). Deep-Sea Res. II, 58, 2678–2694, doi:10.1016/j.dsr2.2010.10.042, 2011.

Koeve, W. and Ducklow, H. W.: JGOFS synthesis and modeling: The North Atlantic ocean, Deep-Sea Res. Part II, 48, 2141–2154, 2001.

Koroleff, F.: Direct determination of ammonia in natural water as indophenol blue, Information on Techniques and Methods for the Seawater Analysis, 1969.

Lannuzel, D., Schoemann, V., de Jong, J., Chou, L., Delille, B., Becquevort, S., and Tison, J.-L.: Iron study during a time series in the western Weddell pack ice, Mar. Chem., 108, 85–95, 2008.

Le Corre, P. and Minas, H. J.: Distribution et evlolution des elements nutritifs dans le secteur indien de l'ocean antarctique en fin de periode estivale, Oceanologica Acta, 6, 365–381, 1983.

Longhurst, A. R.: Large marine ecosystems – patterns, processes and yields, Marine Policy, 15, 377–378, 1991.

Lorrain, A., Savoye, N., Chauvaud, L., Paulet, Y. M., and Naulet, N.: Decarbonation and preservation method for the analysis of organic c and n contents and stable isotope ratios of low-carbonated suspended particulate material, Anal. Chimi. Acta, 491, 125–133, doi:10.1016/s0003-2670(03)00815-8, 2003.
Löscher, B. M.: Relationships among ni, cu, zn, and major nutrients in the southern ocean, Mar. Chem., 67, 67–102, 1999.
Lucas, M., Seeyave, S., Sanders, R., Moore, C. M., Williamson, R., and Stinchcombe, M.: Nitrogen uptake responses to a naturally Fe-fertilised phytoplankton bloom during the 2004/2005 CROZEX study, Deep-Sea Res. II, 54, 2138–2173, 2007.
Lutjeharms, J. R. E. and Vanballegooyen, R. C.: The retroflection of the Agulhas current, J. Phys. Oceanogr., 18, 1570–1583, 1988.
Lutjeharms, J. R. E., Boebel, O., and Rossby, H. T.: Agulhas cyclones, Deep Sea Res., 50, 13–34, 2003.
Marinov, I., Gnanadesikan, A., Toggweiler, J. R., and Sarmiento, J. L.: The southern ocean biogeochemical divide, Nature, 441, 964–967, doi:10.1038/nature04883, 2006.
Martin, J. H.: Glacial-interglacial CO_2 change: The iron hypothesis, Paleoceanography, 5, 1–13, 1990.
Martin, J. H., Gordon, R. M., and Fitzwater, S. E.: Iron in antarctic waters, Nature, 345, 156–158, 1990.
McCartney, M. S.: Subantartic mode water, Transactions-American Geophysical Union, 56, 1011–1011, 1975.
Mohan, R., Mergulhao, L. P., Guptha, M. V. S., Rajakurnar, A., Thamban, M., AnilKurnar, N., Sudhakar, M., and Ravindra, R.: Ecology of coccolithophores in the indian sector of the southern ocean, Marine Micropaleontology, 67, 30–45, doi:10.1016/j.marmicro.2007.08.005, 2008.
Murphy, J., and Riley, J. P.: A modified single solution method for the determination of phosphorus in natural waters, Analytica Chimica Acta, 27, 31–36, 1962.
Nelson, D. M. and Smith, W. O.: Sverdrup revisited – critical depths, maximum chlorophyll levels, and the control of southern ocean productivity by the irradiance regime, Limnol. Oceanogr., 36, 1650–1661, 1991.
Nelson, D. M., Brzezinski, M. A., Sigmon, D. E., and Franck, V. M.: A seasonal progression of si limitation in the pacific sector of the southern ocean, Deep-Sea Res. II, 48, 3973–3995, 2001.

BGD
9, 5011–5048, 2012

Description of the biogeochemical features

F. A. C. Le Moigne et al.

Orsi, A. H., Whitworth, T., and Nowlin, W. D.: On the meridional extent and fronts of the antarctic circumpolar current, Deep-Sea Res. I, 42, 641–673, 1995.
Piola, A. R. and Gordon, A. L.: Intermediate waters in the southwest south-atlantic, Deep-Sea Res. A, 36, 1–16, 1989.
Planchon, F., Cavagna, A.-J., Cardinal, D., André, L., and Dehairs, F.: Late summer particulate organic carbon export and twilight zone remineralisation in the Atlantic sector of the Southern Ocean, Biogeosciences Discuss., 9, 3423–3477, doi:10.5194/bgd-9-3423-2012, 2012.
Pollard, R. T., Lucas, M. I., and Read, J. F.: Physical controls on biogeochemical zonation in the southern ocean, Deep-Sea Res. II, 49, 3289–3305, 2002.
Pondaven, P., Ragueneau, O., Tréguer, P., Hauvespre, A., Dezileau, L., and Reyss, J. L.: Resolving the 'opal paradox' in the southern ocean, Nature, 405, 168–172, 2000.
Quéguiner, B., Tréguer, P., Peeken, I., and Scharek, R.: Biogeochemical dynamics and the silicon cycle in the atlantic sector of the southern ocean during austral spring 1992, Deep-Sea Res. II, 44, 69–89, 1997.
Ragueneau, O., Dittert, N., Pondaven, P., Tréguer, P., and Corrin, L.: Si/c decoupling in the world ocean: Is the southern ocean different?, Deep-Sea Res. II, 49, 3127–3154, 2002.
Ragueneau, O., Chauvaud, L., Moriceau, B., Leynaert, A., Thouzeau, G., Donval, A., Le Loc'h, F., and Jean, F.: Biodeposition by an invasive suspension feeder impacts the biogeochemical cycle of si in a coastal ecosystem (bay of brest, france), Biogeochemistry, 75, 19–41, doi:10.1007/s10533-004-5677-3, 2005.
Reid, J. L.: On the total geostrophic circulation of the south-Atlantic ocean – flow patterns, tracers, and transports, Prog. Oceanogr., 23, 149–244, 1989.
Sarmiento, J. L. and Toggweiler, J. R.: A new model for the role of the oceans in determining atmospheric pCO_2, Nature, 308, 621–624, 1984.
Sarmiento, J. L., Gruber, N., Brzezinski, M. A., and Dunne, J. P.: High-latitude controls of thermocline nutrients and low latitude biological productivity, Nature, 427, 56–60, doi:10.1038/nature02127, 2004.
Smith, K. L., Robison, B. H., Helly, J. J., Kaufmann, R. S., Ruhl, H. A., Shaw, T. J., Twining, B. S., and Vernet, M.: Free-drifting icebergs: Hot spots of chemical and biological enrichment in the weddell sea, Science, 317, 478–482, doi:10.1126/science.1142834, 2007.
Strickland, J. D. H. and Parsons, T. R.: A practical handbook of seawater analysis, Fisheries Research Board of Canada, 2nd edition, 1972.

Tréguer, P. and Jacques, G.: Dynamics of nutrients and phytoplankton, and fluxes of carbon, nitrogen and silicon in the antarctic ocean, Polar Biol., 12, 149–162, 1992.
Tréguer, P. and Le Corre, P.: The ratios of nitrate, phosphate, and silicate during uptake and regeneration phases of the moroccan upwelling regime, Deep Sea Res. A, 26, 163–184, 1979.
Whitworth, T. and Nowlin, W. D.: Water masses and currents of the southern-ocean at the greenwich meridian, J. Geophys. Res.-Oceans, 92, 6462–6476, 1987.
Yool, A., Martin, A. P., Fernandez, C., and Clark, D. R.: The significance of nitrification for oceanic new production, Nature, 447, 999–1002, doi:10.1038/nature05885, 2007.

BGD
9, 5011–5048, 2012

Description of the biogeochemical features

F. A. C. Le Moigne et al.

Table 1. Ranges and comparison of silicate and nitrate concentrations in the upper 200 m water column in several oceanic provinces of the Southern Ocean delimited by the frontal systems at different seasons.

Area	Longitude	Season	[silicate] (µM)	[nitrate] (µM)	[phosphate] (µM)	Reference
North STF	45° E	Jan/Mar	1–6	0–7	0–1.6	Mohan et al. (2004)
	0° E	Feb/Mar	0–5	0–5	0–1.5	This study
STF-SAF	45° E	Jan/Mar	2–10	1–23	0–1.5	Mohan et al. (2004)
	0° E	Feb/Mar	0–5	5–20	0.3–1.6	This study
SAF-PF	6° E	Oct	18–73	24–32	1.2–1.9	Löscher et al. (1997)
	6° E	Nov	1–60	23–35	1.1–2.0	Löscher et al. (1997)
	0° E	Feb/Mar	0–5	15–30	1.2–2.3	This study
PF-SACCF	6° E	Oct	28–82	27–36	1.8–2.3	Löscher et al. (1997)
	6° E	Nov	27–87	27–35	1.9–2.5	
	0° E	Feb/Mar	0–41	25–35	1.6–2.5	This study
SACCF-SBdy	6° E	Oct	28–82	27–36	1.8–2.3	Löscher et al. (1997)
	6° E	Nov	27–87	27–35	1.9–2.5	Löscher et al. (1997)
	0° E	Feb/Mar	41–72	26–35	1.7–2.4	This study

BGD
9, 5011–5048, 2012

F. A. C. Le Moigne et al.

Table 2. Comparison of the estimated daily net production rate of silica (*P*Si, mmol m^{-2} d^{-1}) and nitrate (*P*N, mmol m^{-2} d^{-1}) in the Atlantic sector of the Southern Ocean estimated during the summer 2008 (this study) and in 1994 (Pondaven et al., 2000).

Area	*P*Si (mmol m^{-2} d^{-1})	*P*N (mmol m^{-2} d^{-1})	Reference
SAF-PF	11.9 ± 6.5*	6.6 ± 3.6*	This study
	20.2 ± 4.4	16.1 ± 8.8	Pondaven et al. (2000)
PF-SBdy	21.1 ± 8.8*	6.5 ± 2.9*	This study
	30.3 ± 6.0	13.5 ± 6.7	Pondaven et al. (2000)

* Uncertainties are calculated from the confidence interval of the mean $p < 0.05$.

Discussion Paper | Discussion Paper | Discussion Paper | Discussion Paper |

BGD

9, 5011–5048, 2012

Description of the biogeochemical features

F. A. C. Le Moigne et al.

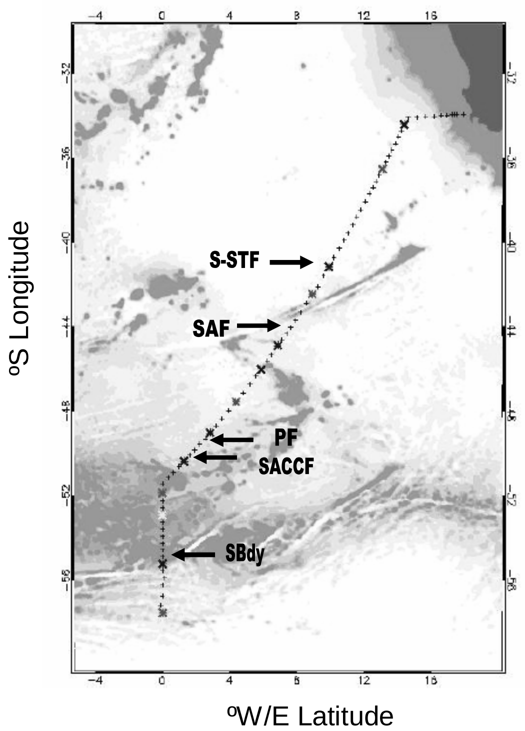

Fig. 1. Location of the stations sampled during the MD166 BONUS-GoodHope cruise. Smaller crosses are for the HYDRO stations, grey crosses the LARGE stations and black crosses the SUPER stations. The positions of fronts are also shown, with the southern branch of the Subtropical Front (S-STF; ∼42°2′ S), the SubAntarctic Front (SAF; 44°2′ S), the Polar Front (PF; 50°22.4′ S), the Southern ACC Front (SACCF; ∼51°52′ S) and the Southern Boundary of the ACC (SBdy; ∼55°54.3′ S).

BGD
9, 5011–5048, 2012

Description of the biogeochemical features

F. A. C. Le Moigne et al.

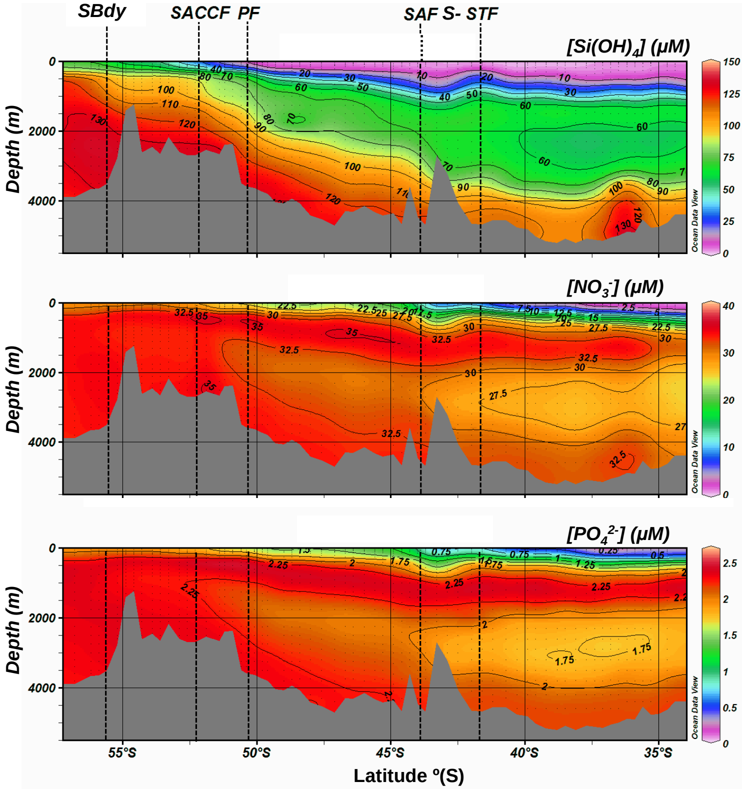

Fig. 2. Contour plots of silicate ($Si(OH)_4^-$; μM), nitrate (NO_3^-; μM), and phosphate (PO_4^{2-}; μM) concentrations versus depth (m) and latitude along the MD166 BONUS-GoodHope section. The colour mapping extrapolation is based on the sampling resolution along the section of ∼2600 km that was achieved with 79 stations separated by ∼15 to 56 km, with a total of 22 sampling depths per station. *Figure from ODV (Reiner Schlitzer).*

BGD

9, 5011–5048, 2012

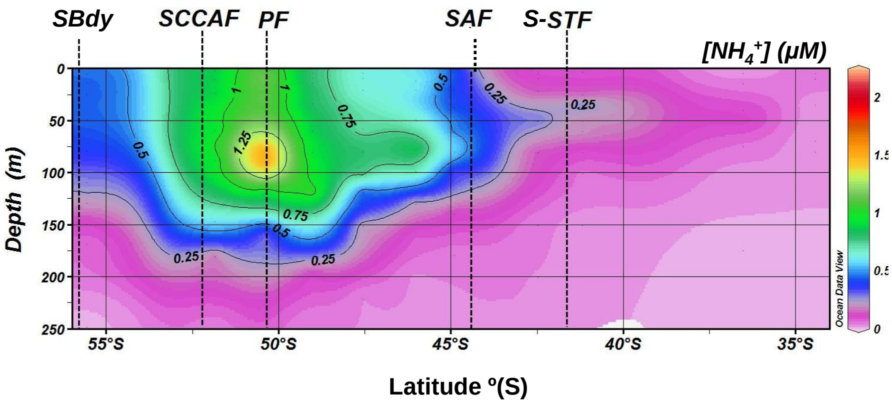

Fig. 3. Contour plot of ammonium concentrations (NH_4^+; µM) in the upper 250 m along the MD166 BONUS-GoodHope section. *Figure from ODV (Reiner Schlitzer)*.

BGD
9, 5011–5048, 2012

Description of the biogeochemical features

F. A. C. Le Moigne et al.

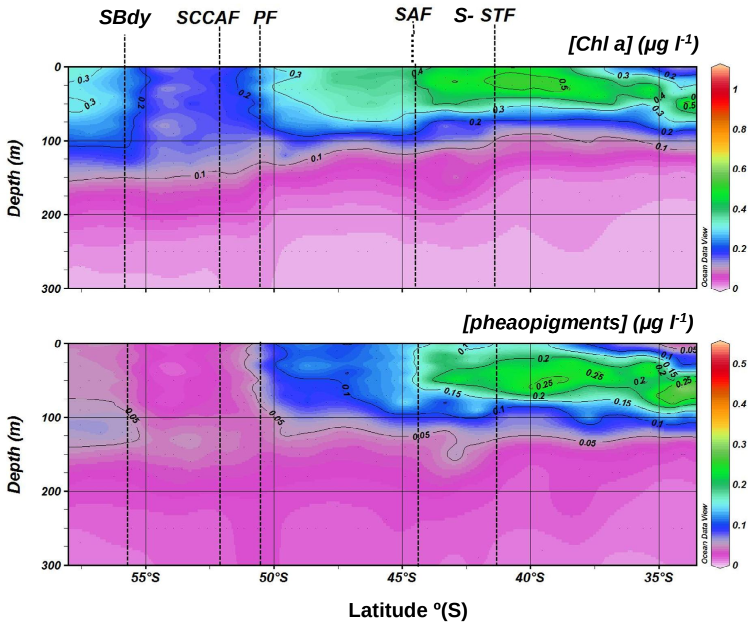

Fig. 4. Contour plots of chlorophyll *a* (chl *a* ; µg l^{-1}) and phaeopigments (phaeopigments; µg l^{-1}) concentrations in the upper 300 m along the MD166 BONUS-GoodHope section. *Figure from ODV (Reiner Schlitzer)*.

BGD

9, 5011–5048, 2012

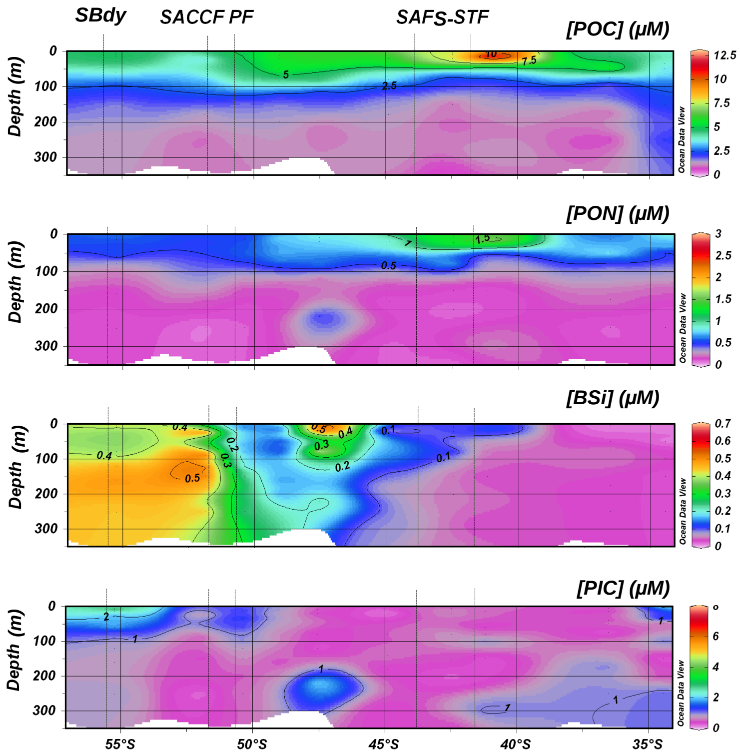

Fig. 5. Contour plots of particulate organic carbon (POC; $\mu mol\ l^{-1}$), particulate organic nitrogen (PON; $\mu mol\ l^{-1}$), biogenic silica (BSi; $\mu mol\ l^{-1}$) and particulate inorganic carbon (PIC; $\mu mol\ l^{-1}$) concentrations in the upper 350 m along the MD166 BONUS-GoodHope section. *Figure from ODV (Reiner Schlitzer)*.

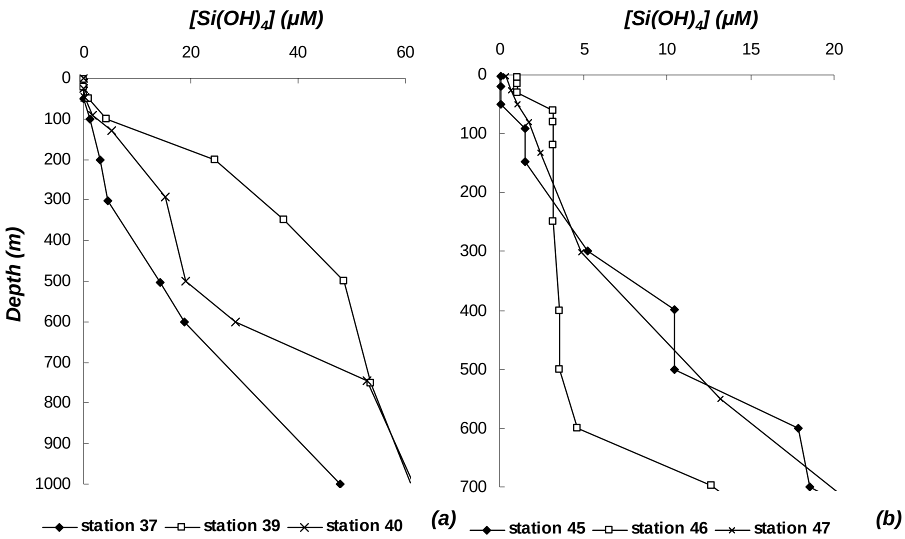

Fig. 6. Vertical distributions of silicate concentrations ($Si(OH)_4^-$; µM), **(a)** in the core of the cyclonic eddy-S (station 39) and the surrounding stations (stations 37 and 40); and **(b)** in the core of the anticyclonic eddy-M (station 46) and the surrounding stations (stations 45 and 47).

BGD
9, 5011–5048, 2012

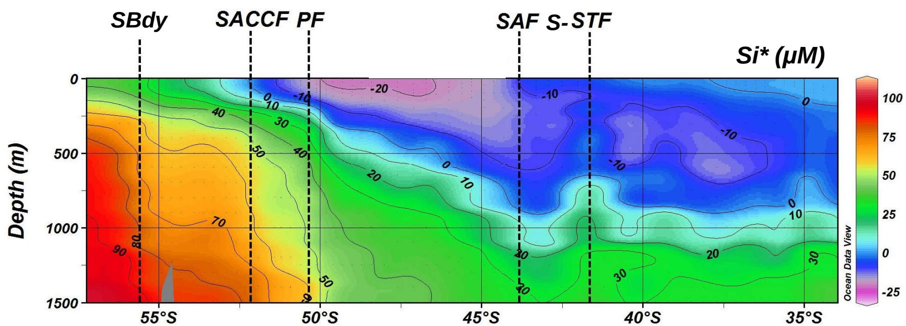

Fig. 7. Contour plot of Si* (defined as [Si]-[NO_3] in μM) Sarmiento et al., 2004) in the upper 1500 m along the MD166 BONUS-GoodHope section. *Figure from ODV (Reiner Schlitzer)*.

BGD
9, 5011–5048, 2012

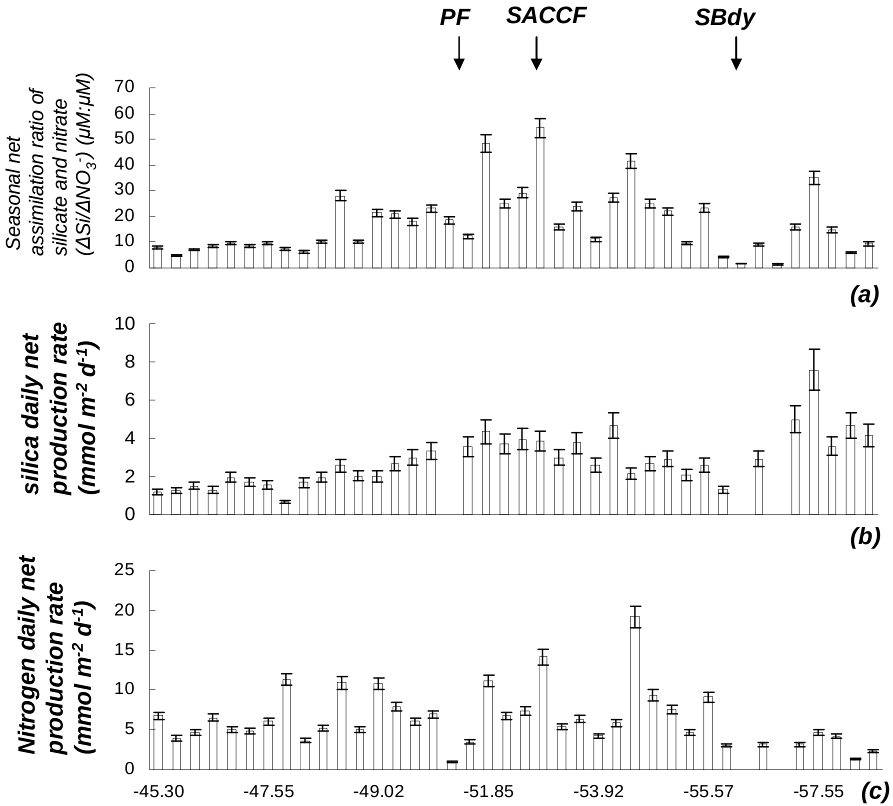

Fig. 8. (a) Seasonal net assimilation ratio of silicate and nitrate ($\Delta Si/\Delta NO_3^-$) in the surface waters in the Antarctic Circumpolar Current (ACC) along the MD-166 BONUS-GOODHOPE cruise (see text for calculation method). Front positions are indicated; **(b)** silica daily net production rate (mmol m^{-2} d^{-1}) and **(c)** nitrogen daily net production rate (mmol m^{-2} d^{-1}) (see text for calculation methods). All the uncertainties are based on observations that nitrate and silicate concentrations in the remnant Winter Waters are within ±7 % of that at the sea surface.

BGD
9, 5011–5048, 2012

Description of the biogeochemical features

F. A. C. Le Moigne et al.

Title Page
Abstract | Introduction
Conclusions | References
Tables | Figures
◀| |▶
◀ ▶
Back | Close
Full Screen / Esc
Printer-friendly Version
Interactive Discussion